

THE DOUBLE INTERPOLATION AND DOUBLE PREDICTION (DIDP) APPROACH FOR INSAR AND GPS INTEGRATION

Linlin Ge, Shaowei Han, and Chris Rizos

School of Geomatic Engineering
The University of New South Wales
Sydney, Australia

KEY WORDS: Synthetic Aperture Radar Interferometry, Global Positioning System, Crustal Deformation.

ABSTRACT

The technique of synthetic aperture radar interferometry (or InSAR) was first suggested in 1974. Due to its characteristics of very high spatial resolution and wide coverage, as well as the cost effectiveness of the technique, it is not surprising that many earthquake ruptures have been studied using InSAR. However, InSAR is very sensitive to errors such as atmospheric effects, satellite orbit error, the condition of the ground surface and temporal decorrelation. Furthermore the repeat cycle of 35 (ERS-1) to 44 (JERS-1) days for SAR satellites cannot provide sufficient temporal resolution for some applications. On the other hand, many Continuous GPS (CGPS) networks of receivers have been established in recent years. CGPS can provide temporally dense observations (e.g. sampling at an interval of 30 seconds or higher), but these GPS receivers, spaced at about 25km apart for the densest arrays, are not spatially dense enough to characterise the dynamics of seismic faults. These require sub-kilometre level spatial resolution. Therefore, the two techniques of InSAR and CGPS appear to be very complementary.

The proposed Double Interpolation and Double Prediction (DIDP) approach can be used to integrate InSAR and GPS results. The first step is to derive atmospheric corrections to the InSAR images from CGPS data, using techniques borrowed from 'GPS meteorology'. The second step is to remove or mitigate SAR satellite orbit errors by using the GPS results as constraints. These atmospheric and orbit corrections generate a GPS-corrected InSAR result. In the third step, the CGPS observations separated by one or several InSAR repeat cycles are densified in a grid manner by interpolation in the spatial domain, based on the GPS-corrected InSAR results; and then the densified grid observations are interpolated in the time domain using the daily, hourly, or even 30 second sampling rate of the CGPS time series. In the fourth step, based on the double interpolation result of the third step, forward filtering is used to predict the crustal deformation at all points on the grid. This is in fact a double prediction in both the temporal and spatial domains.

Some algorithms and preliminary results of the DIDP technique for integrating InSAR and GPS results will be presented in this paper.

1 INTRODUCTION

Interferometric synthetic aperture radar (InSAR) is a technique suggested first in 1974 (Graham, 1974). Topographic change measurement by InSAR was first demonstrated for Seasat L-band data (Gabriel et al. 1989), and later with the spectacular contour map of coseismic deformation associated with the 1992 Landers earthquake in southern California obtained with the ERS-1 data (Massonnet et al., 1993).

Due to its very high spatial coverage and cost effectiveness many earthquakes have been studied with InSAR (e.g., Fujiwara et al., 1997). Moreover, InSAR enjoys around 25m spatial resolution on the ground. But InSAR is very sensitive to errors such as atmospheric effects, satellite orbit error, condition of ground surface and temporal decorrelation. When present in the InSAR image these errors can lead to misleading results and there appears to be no way to eliminate them using only SAR data. Furthermore the repeat cycle of 35 to 44 days of SAR satellites cannot provide enough temporal resolution for applications such as distinguishing deformations before, during, and after earthquakes or volcanic activity.

Many continuous Global Positioning System (CGPS) networks of receivers have been set up in recent years. Data from CGPS arrays are also used for meteorological research to map tropospheric water vapour and to detect ionospheric disturbances. Most CGPS arrays are now sampling at an interval of 30 seconds. Therefore CGPS can provide (temporally) very dense observations. But these CGPS arrays are not spatially dense enough for monitoring seismic faults, which may require sub-km level spatial resolution. For example, the GEONET in Japan, currently the densest CGPS array in the world, has inter-receiver spacing of the order of 25km.

If the two techniques are compared further, GPS results (with the support of Satellite Laser Ranging and Very Long Baseline Interferometry) can be considered as being in relation to an 'absolute' reference system. On the other hand, while assuming that there are no displacements at a few reference points in a radar image in data processing, InSAR results are essentially 'relative' measurements. GPS measurements on the reference points in a SAR image can also be used as constraints to mitigate the influence of SAR satellite orbit errors. However, InSAR results, with their high spatial resolution, can be used to greatly densify GPS observations in the spatial sense. Therefore, the two techniques are very complementary.

The idea of InSAR and GPS integration was perhaps first suggested in 1997 (Bock et al. 1997). The Double Interpolation and Double Prediction (DIDP) approach for this integration was first proposed in 1997 (Ge et al. 1997). Some algorithms and results of DIDP are discussed in this paper.

2 DERIVING ATMOSPHERIC CORRECTION TO INSAR FROM CGPS

In the DIDP approach the first step is to derive atmospheric corrections to InSAR using CGPS data, which benefits greatly from the efforts of 'GPS meteorology' (Bevis et al, 1992).

It is well-known that the accuracy of InSAR measurement is limited mostly by atmospheric propagation heterogeneity (due to the highly variable distribution of atmospheric water vapour) in space and time (e.g. Massonnet et al, 1995). Atmospheric refraction artefacts in the InSAR result may introduce errors as large as three fringes locally, in the case of exceptional conditions. Therefore they have to be corrected before InSAR results can be used for deformation monitoring.

On the other hand, although the primary purpose of almost all CGPS arrays is to address geodetic applications, they may also produce estimates of the tropospheric zenith delay in the immediate vicinity of the GPS station as a byproduct of data processing (in the process of stochastic estimation associated with atmospheric modelling). Using CGPS data it is possible to map the tropospheric zenith delay with high resolution in both space and time. This, in turn, can be used as an atmospheric 'correction' to the InSAR result. There is good reason to assume that such atmospheric 'corrections' generated from CGPS data will soon be generally available, as there is a growing interest in the monitoring of atmospheric water vapour.

Water vapour is one of the most significant constituents of the atmosphere since it is the means by which moisture and latent heat are transported to cause "weather". Water vapour is also a greenhouse gas that plays a critical role in the global climate system. Despite its importance to atmospheric processes over a wide range of spatial and temporal scales, water vapour is one of the least understood and poorly described components of the Earth's atmosphere.

While an important goal in modern weather prediction is the improvement of short-term cloud and precipitation forecasts, the ability to do so is severely limited by the lack of timely and accurate water vapour information. Traditional water vapour observing systems include radiosondes, surface-based radiometers, satellite-based radiometers, and some research aircraft. Each of these systems has advantages and limitations. Although it also has limitations, many researchers believe that ground-based CGPS will be most useful as an element of a composite upper-air observing system. In this role it will provide frequent water vapour measurements to constrain numerical weather prediction models, as well as independent calibration and validation of satellite measurements.

The principle of using GPS data to measure water vapour is based on the fact that GPS radio signals are slowed as they propagate from the GPS satellites to ground-based receivers, passing through layers of the Earth's atmosphere: the ionosphere and the neutral atmosphere. This slowing delays the arrival time of the transmitted signal from that expected if there were no intervening media. It is possible to correct for the ionospheric delay, which is frequency dependent, by using dual-frequency GPS receivers. The delays due to the neutral atmosphere, however, are effectively non-dispersive at GPS frequencies and so cannot be corrected in this way. They depend on the constituents of the atmosphere, which are a mixture of dry gases and water vapour.

In a ground-based GPS system, the signal delays from several (at least four, but typically 6 or more) satellites in view are simultaneously measured. These delays are mathematically adjusted (scaled) such that all satellite signals are treated as having been transmitted from directly overhead (at the zenith) simultaneously, using the mapping function:

$$M_T(\theta) = 1/\sin \theta \quad (2.1)$$

where θ is the elevation angle from receiver to the satellite. The averaged vertically-scaled signal delay introduced by the atmospheric constituents is called the Zenith Total (or Tropospheric) Delay (ZTD). ZTD can be separated into two components, the zenith hydrostatic delay (ZHD) and the zenith wet delay (ZWD):

$$\Delta L = \Delta L_h^0 M_h(\mathbf{q}) + \Delta L_w^0 M_w(\mathbf{q}) \quad (2.2)$$

where $M_h(\mathbf{q})$ and $M_w(\mathbf{q})$ are the hydrostatic and wet mapping functions respectively. ΔL_h^0 and ΔL_w^0 are ZHD and ZWD respectively (in mm).

The ZHD is calculated by measuring the surface pressure and applying a mapping function. The ZWD can be viewed as a stochastic process, and the process parameters can be estimated using a Kalman filter. In fact, both stochastic and deterministic algorithms for atmospheric modeling are employed in high precision GPS software such as GIPSY, GAMIT and the Bernese package.

Suppose the ZTD at GPS station i at the SAR image acquisition time t is $\Delta L_i(t)$ using Eqn. (2.2), the atmospheric correction derived from GPS data to the InSAR result on the image point of station i should be:

$$\mathbf{d}_i = \Delta L_i(t_2) - \Delta L_i(t_1) \quad (2.3)$$

where t_1 and t_2 correspond to the imaging time of the two SAR images used in the interferometric processing. The atmospheric correction for other image points can be interpolated from the GPS stations.

3 REMOVE OR MITIGATE SAR SATELLITE ORBIT ERRORS BY USING GPS RESULTS AS CONSTRAINTS

The second step of DIDP is to remove or mitigate SAR satellite orbit errors by using GPS results as constraints. For this purpose, metal corner reflectors can be co-located with, or 'tied' precisely to, some GPS sites on the ground. The SAR data covering each of these GPS sites thus correspond to a precisely-located point, and hence could be used to provide 3-D corrections to the spacecraft orbit, and improve hence the accuracy of the ground displacement measurement.

Fig.1 illustrates the InSAR geometry. The radar beam is transmitted to the ground from antenna A_1 . After scattering at the ground point G , the radar wave is received by antennas at both A_1 and A_2 . The distance between A_1 and A_2 (the baseline length) is B (exactly 60m in the case of the Shuttle Radar Topography Mission (SRTM), the length of the mast (JPL, 1999)) and the radar look angle is θ . The GPS heights of the antenna A_1 and the ground point G are H and h respectively. H can be estimated from the SAR satellite ephemeris, but usually not precisely enough for deriving DEM or deformation information (because it is one of the orbit errors to be mitigated), although for SRTM data it is precisely known because GPS receivers were flown aboard the space shuttle. The h is usually an unknown to be solved by InSAR but is known precisely if a GPS receiver and corner reflector are employed at the control point. Suppose $\beta = \angle G A_1 A_2$ can be calculated from the orientation of the baseline, then the geometric distance r between A_1 and G can be calculated as:

$$r = \frac{B^2 - d^2}{2d + 2B \cos b} \quad (3.1)$$

where δ can be calculated from the phase difference φ from InSAR as:

$$d = \frac{j}{2p} \lambda \quad (3.2)$$

where λ is the radar wavelength. Therefore, the SAR vehicle height estimated from the ground control point information is:

$$H = h + r \cos \varphi \quad (3.3)$$

Several estimations of H can be obtained if there are several ground control points. By giving different weights to both these estimates and the H derived from the SAR satellite ephemeris in a least-squares process (Giordano & Hsu, 1985), the orbit errors can be effectively reduced.

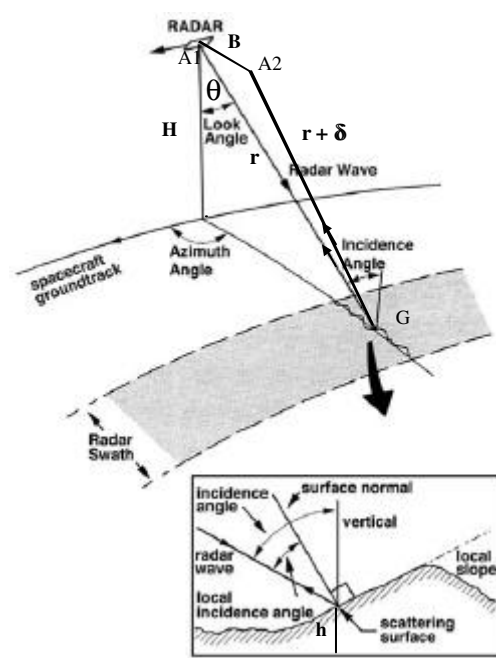


Figure 1. The radar interferometry geometry.

4 DENSIFY OBSERVATIONS BY DOUBLE INTERPOLATION

The atmospheric and orbit corrections dealt with in the previous two sections yield GPS-corrected InSAR results. In the third step of DIDP, the CGPS observations separated by one or several InSAR repeat cycles are densified in a grid manner by interpolation in the spatial domain based on the GPS-corrected InSAR results (geophysical information has been incorporated in the distribution model for this interpolation) (Ge et al, 1999). Then the densified grid observations are interpolated in the time domain based on the daily, hourly, or even 30 second sampling rate CGPS time series (adaptive filtering based on the least-mean-square algorithm has been used to extract the dynamic model for this interpolation) (Ge, 1999).

4.1 Distribution Model For Interpolation Based on InSAR Result and Incorporating Geophysical Information

To start the interpolation process, an irregular grid pattern is formed based on the locations of the stations in the GPS network. As shown in Fig. 2, the latitudes and longitudes of the GPS stations are read from a data file. The latitudes and longitudes are then sorted according to their values. The sorted latitudes and longitudes are then combined to form the grid, consisting of both existing GPS stations (denoted by “G”) and points to be interpolated (denoted by “I”). The important feature of this two-dimensional sorting is that the attributes of the GPS stations are maintained so that no interpolation operation is needed on grid points of GPS stations. Therefore, the algorithm carries out “indexed sorting”. It can be seen from Fig.2 that there is one and only one GPS station in both the rows and the columns on the transformed grid. In practical applications, however, there may be two or more when the CGPS array is very dense and some of the stations are very close, or in the contrary situation, there may be none in a row or column when the CGPS array is very sparse but a relatively dense 'densification' is desired.

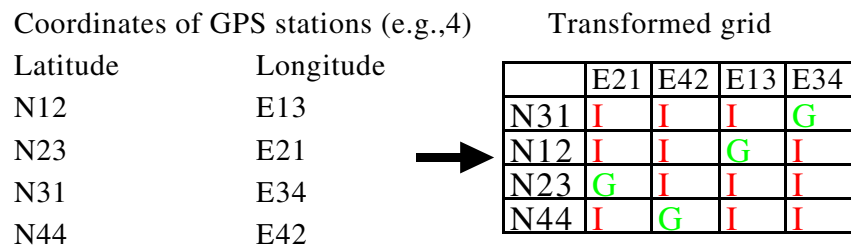


Figure 2. An irregular grid formed by indexed sorting.

In order to interpolate objectively, it is proposed that geophysical information be incorporated. It is well known that the movements of GPS stations on the two sides of a fault can be significantly different, therefore it is important to classify the stations and the intended interpolating points according to their positions in relation to the fault. The open- (Fig. 3) and closed- (Fig. 4) curve models have been designed to describe the geometric characteristics of faults. In the open-curve model, as shown in Fig. 3, the region of interest is divided into upper (or left) and lower (or right) sub-regions by an open curve. This model should be adequate for most seismic faults.

An algorithm has been developed to automatically identify in which sub-region a station or an interpolating point belongs to. Assume the unit vectors of latitude is \vec{i} and longitude is \vec{j} , from an arbitrary point on the fault (N_i, E_i) to the GPS station (GS) at (N_G, E_G) the vector can be expressed as:

$$\vec{G} = (N_G - N_i) \bullet \vec{i} + (E_G - E_i) \bullet \vec{j} \tag{4.1}$$

A minimum search of vector length is performed to find $|\vec{G}|_{(N_i, E_i)} = \min$

Therefore, a GS local fault vector can be written as:

$$\vec{F}_G = (N_{i+1} - N_i) \bullet \vec{i} + (E_{i+1} - E_i) \bullet \vec{j} \tag{4.2}$$

From an arbitrary point on the fault (N_j, E_j) to the interpolating point (IP) at (N_I, E_I) the vector can be expressed as:

$$\vec{I} = (N_i - N_j) \bullet \vec{i} + (E_i - E_j) \bullet \vec{j} \tag{4.3}$$

A minimum search of vector length is performed to find $|\vec{I}|_{(N_j, E_j)} = \min$

Then, an IP local fault vector can be written as:

$$\vec{F}_I = (N_{j+1} - N_j) \bullet \vec{i} + (E_{j+1} - E_j) \bullet \vec{j} \tag{4.4}$$

From Eqns. (4.1) to (4.4) a “decision” can be made: if $(\vec{F}_G \times \vec{G}) \bullet (\vec{F}_I \times \vec{I}) > 0$ the GPS station and the interpolating point are on the same side of the fault. Otherwise they are on different sides of the fault.

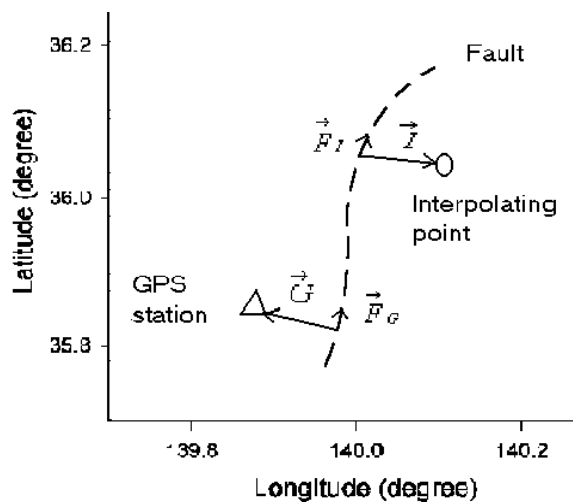


Figure 3. Open-curve model: one GPS station and one interpolating point case.

In the closed-curve model, as shown in Fig. 4, the region to be studied is divided into 'outside' and 'inside' sub-regions by a closed curve. This model is appropriate for applications such as volcano deformation monitoring.

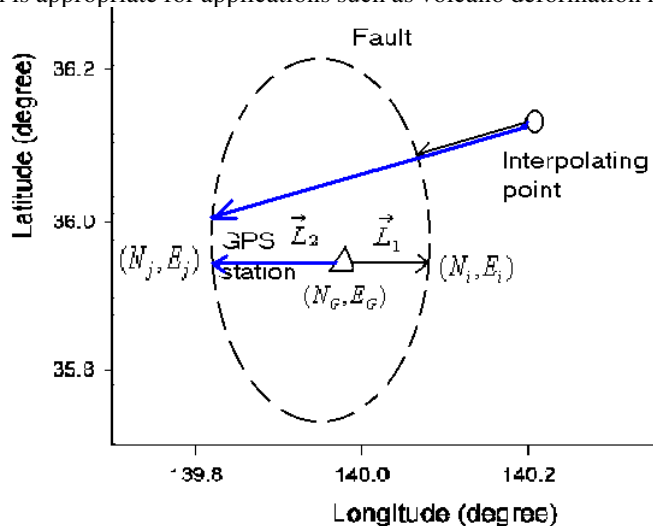


Figure 4. Closed-curve model: one GPS station and one interpolating point case.

A different algorithm for this model is developed to automatically identify in which sub-region a station or interpolating point belongs to. Again assume the unit vectors of latitude is \vec{i} and longitude is \vec{j} . From the GPS station (GS) at (N_G, E_G) to an arbitrary point on the fault (N_i, E_i) the vector can be expressed as:

$$\vec{G} = (N_i - N_G) \bullet \vec{i} + (E_i - E_G) \bullet \vec{j}$$

A minimum search of vector length is performed to find $|\vec{G}|_{(N_i, E_i)} = \min$

The GS primary vector is thus determined as: $\vec{L}_1 = \vec{G}$ (4.5)

Then a minimum distance search from an arbitrary point on the fault to the GS primary vector can determine (N_j, E_j) , which is used to calculate the GS secondary vector:

$$\vec{L}_2 = (N_j - N_G) \bullet \vec{i} + (E_j - E_G) \bullet \vec{j} \tag{4.6}$$

From Eqns. (4.5) and (4.6), a “decision” can be made: if $\vec{L}_1 \bullet \vec{L}_2 > 0$ the GPS station is outside of the fault. Otherwise it is inside the fault. The position of the interpolating point relative to the fault can be determined in the same way.

The combination of open- and closed-curve models can deal with comparatively complex fault systems.

After the classification of GPS stations and the intended interpolating points into different groups, a distribution model for interpolation for each group based on the GPS-corrected InSAR results is proposed, as illustrated in Table 1. In some sites of interest (Sites 1 to 4) there are both GPS and InSAR results for the deformation (the CGPS results may have to span one or more InSAR repeat cycles depending on the availability of suitable SAR image pairs). But in most other sites (Sites 5, 6, ...) there will only be InSAR-derived results. All of the results are input into a least-squares adjustment (e.g. Giordano & Hsu, 1985). The adjusted results, which form the distribution model for interpolation in spatial domain, are used as constraints later on to scale the time series generated at the interpolated points based on the dynamic model.

Table 1. Distribution model based on InSAR information

Interested Site	GPS Result	InSAR result	Least-square adjusted result
1	G1	S1	A1
2	G2	S2	A2
3	G3	S3	A3
4	G4	S4	A4
5		S5	A5
6		S6	A6

It is important to have overlapping GPS and InSAR results over the active fault region so that the GPS results can be used to calibrate out some errors in the InSAR results. But this condition is very hard to satisfy (Bock & Williams, 1997). It is hoped that the densification of CGPS and new missions for InSAR such as the Shuttle Radar Topography Mission (SRTM), Airborne Synthetic Aperture Radar (AIRSAR), Geographic Synthetic Aperture Radar mission (GeoSAR), and Lightweight Synthetic Aperture Radar (LightSAR) (JPL, 1999), will ease such difficulties.

4.2 Dynamic Model For Interpolation Based on CGPS Times Series

After the classification of GPS stations and the intended interpolating points into different groups, CGPS results sampled daily, hourly, or even every 30 second from stations in the same sub-region are used to derive a dynamic model, which is used to interpolate in the time domain at grid points in the same sub-region. Fig. 5 is an example of a dynamic model extracted using an adaptive filter based on the least-mean-square algorithm (Ge, 1999) for daily CGPS results from two closely located stations in the same classified group: stations BRAN and LEEP of the SCIGN. After the filtering, the primary input (top plot in the figure) has been separated into the extracted dynamic model (second plot from the bottom in the figure), which is the coherent component to the reference input, and the local movement (bottom plot in the figure), which is the incoherent component to the reference input. If there is only one CGPS station in the sub-region, its time series is used directly as the dynamic model. If there are more than two CGPS stations in the same sub-region, one of them is used as the primary station and the others are used to provide reference sequences and the adaptive filter is

extended to handle a single primary input and multiple reference inputs system, rather than the single reference input system as shown in Fig. 5.

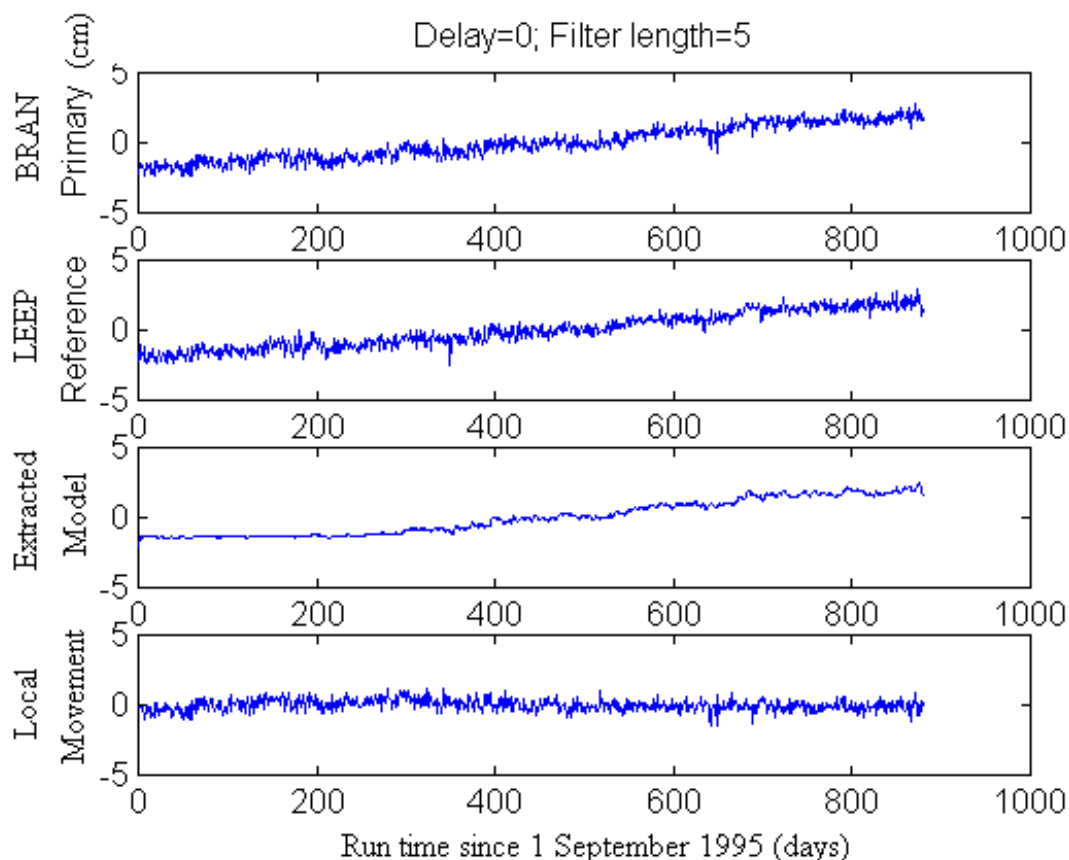


Figure 5. Dynamic model extracted using adaptive filtering on CGPS results from BRAN and LEEP stations of SCIGN (latitude component, data courtesy of Jet Propulsion Laboratory, NASA, USA).

After the double interpolation in this step, deformations at the GPS sites and interpolated points are both spatially and temporally dense enough to be used to prepare an 'animation' of how the crust deforms.

5 EXTRAPOLATE QUASI-OBSERVATIONS BY DOUBLE PREDICTION

In the fourth step of DIDP, based on the double interpolation result (quasi-observations) of the third step, forward filtering (Kalman filtering) is used to predict the crustal deformation at all points on the grid. This is in fact a double prediction in both the time and spatial domains, which could facilitate the use of the DIDP technique for applications such as the prediction of volcano eruption or earthquake ruptures. Moreover, this step is very important in the three-step reliability test (RT) for DIDP. In the first step of RT, the CGPS and SAR data are processed to yield a CGPS time series and the InSAR image respectively. In the second step of RT, the CGPS time series from some of the sites are used together with the InSAR image in the double interpolation to predict CGPS time series for the rest of the CGPS sites. The CGPS time series for these latter sites, from both observation and prediction, are compared to test the reliability of the double interpolation. In the third step of RT, the CGPS time series from all the sites in one SAR repeat cycle are used, together with the InSAR image for the same SAR repeat cycle in the double interpolation, to generate quasi-CGPS time series for all the points on a grid. These quasi-CGPS time series are then used in the double prediction to yield the deformation in the next SAR repeat cycle. The predicted deformation is compared with the CGPS and InSAR results in the next repeat cycle to further test the reliability of the double prediction.

6 CONCLUDING REMARKS

The Double Interpolation and Double Prediction (DIDP) approach for integrating InSAR and GPS results has been presented in this paper. In the DIDP approach, the first step is to derive the atmospheric corrections to InSAR from the

CGPS measurements. The second step is to remove or mitigate the SAR satellite orbit errors by using GPS results as constraints. Metal corner reflectors are co-located with (or tied precisely to) some GPS sites. The SAR data covering each of these GPS sites thus correspond to a precisely-located point, and hence could be used to provide 3-D corrections to the spacecraft orbit, hence improving the accuracy of the ground displacement measurement. These atmospheric and orbit corrections yield GPS-corrected InSAR results. In the third step, the CGPS observations separated by one or several InSAR repeat cycles are densified in a grid by interpolation in the spatial domain based on the GPS-corrected InSAR results. Then the densified grid observations are interpolated in the time domain based on the daily, hourly, or even 30 second sampling rate of the CGPS time series. In the fourth step, based on the double interpolation result of the third step, forward filtering (using a Kalman filter) is used to predict the crustal deformation at all points on the grid, which is in fact a double prediction in both the time and spatial domains.

Since a single SAR image usually covers an area of only 50km by 50km, the reliability of spatial interpolation is guaranteed. Because GPS receivers are operating continuously, and can achieve high accuracy, the DIDP method is a promising strategy for significantly improving the spatial, temporal and magnitude resolution of ground deformation monitoring.

ACKNOWLEDGEMENTS

The first author is supported by an International Postgraduate Research Scholarship. This study is partly sponsored by a grant from the Australian Research Council.

REFERENCES

- Bevis, B.G., S. Bussinger, T.A. Herring, C. Rocken, R.A. Anthes, and R.H. Ware, 1992. GPS Meteorology: Remote Sensing of Atmospheric Water Vapor Using the Global Positioning System, *J. Geophys. Res.*, 97, 15787-15801.
- Bock, Y. and S. Williams, 1997. Integrated Satellite Interferometry in Southern California, *EOS Trans., AGU*, Vol.78, No.29, page 293.
- Fujiwara, S., M. Tobita and M. Murakami, 1997. Detecting Crustal Deformation and Generating Digital Elevation Model Using Interferometric Synthetic Aperture Radar, *Jour. Japan Soc. Photogram. Remote Sensing*, Vol.36, No.3, (in Japanese).
- Gabriel, A.K., R.M. Goldstein, and H.A. Zebker, 1989. Mapping Small Elevation Changes Over Large Areas: Differential Radar Interferometry, *J. Geophys. Res.* Vol.94, No.B7, 9183-9191.
- Ge, L., Y. Ishikawa, S. Fujiwara, S. Miyazaki, and X. Qiao, 1997. The Integration of InSAR and CGPS: A Solution to Efficient Deformation Monitoring, *Int. Symp. on Current Crustal Movement and Hazard Reduction in East Asia and South-east Asia*, Wuhan, P.R. China, 4-7 November.
- Ge, L., S. Han, and C. Rizos, 1999. Interpolation of GPS Results Incorporating Geophysical and InSAR Information, *Int. Symp. on GPS - Application to Earth Sciences & Interaction with Other Space Geodetic Techniques*, 18-22 October, Tsukuba, Japan.
- Ge, L., 1999. GPS Seismometer and its Signal Extraction, the Satellite Division of the Institute of Navigation 12th International Technical Meeting (ION GPS '99), 14-17 September, Nashville, Tennessee.
- Giordano, A. and F. Hsu, 1985. *Least Square Estimation with Applications to Digital Signal Processing*. New York, Wiley, 412pp.
- Graham, L.C., 1974. Synthetic Interferometer Radar for Topographic Mapping, *Proc. IEEE*, Vol.62, 763-768.
- JPL, 1999. <http://www.jpl.nasa.gov/missions/>
- Massonnet, D., M. Rossi, C. Carmona, F. Adragna, G. Peltzer, K. Feigl, and T. Rabaute, 1993. The Displacement Field of the Landers Earthquake Mapped by Radar Interferometry, *Nature*, Vol.364, No.6433, 8, 138-142.
- Massonnet, D., P. Briole, and A. Arnaue, 1995. Deflation of Mount Etna Monitored by Spaceborne Radar Interferometry, *Nature*, Vol.375, 567-570.